

# Miniaturised silicon biosensors for the detection of triglyceride in blood serum†

Cite this: *Anal. Methods*, 2014, 6, 1728

Mohanasundaram Sular Veeramani,<sup>a</sup> Karuppiyah Prakash Shyam,<sup>b</sup>  
Noel Prashant Ratchagar,<sup>a</sup> Anju Chadha<sup>bc</sup> and Enakshi Bhattacharya<sup>\*a</sup>

This paper reports on the design and fabrication of electrolyte insulator semiconductor capacitor (EISCAP) devices to detect triglycerides in the form of microreactors fabricated by bulk micromachining of silicon. We have developed a complete triglyceride biochip wherein the enzyme for hydrolysis and the counter electrode for signal transduction are integrated with a miniaturised EISCAP sensor. A compact readout system that measures the triglyceride concentration in blood serum under test has been developed and is implemented in a Programmable System on Chip (PSoC®). The miniaturised EISCAP devices are tested using blood serum samples to estimate the triglyceride concentration within the clinical range of 50 to 150 mg dL<sup>-1</sup> and the time taken by the readout system to calibrate the sensor and to measure the triglyceride is less than 5 minutes.

Received 19th December 2013  
Accepted 19th December 2013

DOI: 10.1039/c3ay42274g

[www.rsc.org/methods](http://www.rsc.org/methods)

## 1 Introduction

Silicon is a well known material that is being used for a wide variety of application-specific sensor systems.<sup>1</sup> A biosensor based on silicon can be of low cost when mass produced. Silicon biosensors can be miniaturised and used with sample volumes as low as a few microliters. Our motivation in this work is to design a silicon biochip that allows fast and direct determination of triglycerides within the clinical measurement range. Triglycerides (TGs), which are present in the form of fats in food as well as in the human body, are important to monitor as high blood TG levels are indicative of high risk of cardiovascular problems. Presently, TG levels are estimated using spectrophotometric methods wherein the instrumentation is complex and expensive, making it essential to develop simple and inexpensive biosensors. Various types of TG biosensors such as electrochemical,<sup>2</sup> amperometric<sup>3-5</sup> and potentiometric,<sup>2</sup> and those using conducting polymer<sup>2</sup> and nanoparticles<sup>2</sup> have been reported recently. Many silicon biosensors work on the principle of impedance or change in the surface charge when they come in contact with electrolytes and thereby develop a

potential across the semiconductor-liquid interface and are classified as potentiometric biosensors.<sup>6-10</sup> Ion Sensitive Field Effect Transistors (ISFETs) and electrolyte insulator semiconductor capacitors (EISCAPs)<sup>11,12</sup> are such types of silicon based sensors used in the determination of bio-analytes like TG and urea through an enzymatic reaction. ISFET and EISCAP devices resemble the structure of Metal Oxide Semiconductor Field Effect Transistors (MOSFETs) and metal oxide semiconductor capacitors (MOSCAPs) respectively. The advantage of ISFET sensors is the relative simplicity of design of readout electronics, since the ISFET drain current which is a function of pH can be readily converted into a voltage. On the other hand, EISCAPs have the advantage of easy fabrication and are more robust. The capacitance-voltage ( $C-V$ ) characteristics of EISCAPs get modulated depending upon the pH of the electrolyte. In the presence of the enzyme lipase, the triglyceride (bio-analyte) is hydrolysed and there is a change in the pH of the electrolyte that shows up as a shift in the  $C-V$  plot.<sup>13,14</sup> Thus, from the shift in the  $C-V$  plot, the amount of TG being hydrolysed can be determined. We have previously reported on the working of large EISCAP sensors made on silicon to detect triglyceride and urea.<sup>15-18</sup> Miniaturised EISCAPs have been fabricated using bulk micromachining of silicon and have been used to sense tributyrin (a short-chained triglyceride).<sup>17</sup> Direct readout circuits to calibrate the sensor against process variations and to measure the pH under test have been developed for a large sized EISCAP and a miniaturised EISCAP.<sup>19,20</sup> For the EISCAP sensors we have used a stacked gate dielectric layer of silicon oxide and silicon nitride. While the oxide ensures a better interface with silicon, the silicon nitride layer has better pH sensitivity and is more resistant to electrolyte spoiling. In this paper, we discuss the design and implementation details of

<sup>a</sup>Department of Electrical Engineering, Indian Institute of Technology Madras, Chennai 600036, India. E-mail: [enakshi@ee.iitm.ac.in](mailto:enakshi@ee.iitm.ac.in); Fax: +91 44 2257 4402; Tel: +91 44 2257 4419

<sup>b</sup>Department of Biotechnology, Indian Institute of Technology Madras, Chennai 600036, India

<sup>c</sup>National Center for Catalysis Research, Indian Institute of Technology Madras, Chennai 600036, India

† Electronic supplementary information (ESI) available: A text file discussing (1) detailed process steps with schematics of miniaturised EISCAPs, (2) enzyme assay and characterisation and (3) principle and design of a pH readout system. See DOI: 10.1039/c3ay42274g

the miniaturised EISCAP along with the readout circuit as a fully functional triglyceride sensor in clinical applications.

## 2 Materials and methods

Triglyceride biosensors are fabricated using 400  $\mu\text{m}$  thick 3'' p-type 1–10  $\Omega\text{ cm}$  single side polished crystalline silicon (100) wafers and 500  $\mu\text{m}$  thick 4'' boro-float glass wafers. The wafer cleaning and processing chemicals such as sulphuric acid, hydrogen peroxide, ammonium hydroxide, hydrochloric acid, hydrofluoric acid, potassium iodide, iodine, ammonium ceric nitrate, acetic acid, ethanol, aminopropyltriethoxysilane (APTES), toluene, glutaraldehyde, tributyrin, Tris-HCl buffer, phosphate buffer, acetonitrile, and *p*-nitro phenol butyrate (*p*NPB) are purchased from Sigma Aldrich, India. Lipase from *Pseudomonas cepacia* is purchased from Amano, Japan. Buffer and other solutions are prepared using DI water of 18.2 M $\Omega\text{ cm}$  resistivity.

### 2.1 Sensor fabrication

The sensors are fabricated using processes similar to those reported previously by us.<sup>20,21</sup> Briefly, the silicon wafer after cleaning using a standard RCA cleaning procedure are bulk micromachined to a depth of 100  $\mu\text{m}$  within masking silicon dioxide windows of dimensions 1.5 mm  $\times$  1.5 mm. The miniaturised microreactors are electrically isolated from each other by a field oxide. In each microreactor, a 10 nm thin layer of gate oxide is grown in a rapid thermal oxidation (RTO) system (AnnealSys, France) and 30 nm of gate nitride is deposited in a plasma enhanced chemical vapor deposition (PECVD) system (Oxford Plasma Technology, UK). Aluminium is deposited on the rear side of the sensor for back contact after removing any residual oxide and nitride insulation. A detailed explanation of the sensor fabrication is given in the ESI.†

### 2.2 TG sensor fabrication

In the above sub-section, fabrication of a pH sensor is discussed where the gate nitride is a pH sensitive layer. This sensor becomes a TG sensor only after making it specific to detect TG by covalently immobilising the bioreceptor lipase to the surface of the sensor. The enzyme (lipase) with amine ( $-\text{NH}_2$ ) terminations can be covalently attached to a molecular layer that has the same amine ( $-\text{NH}_2$ ) terminations using a linker molecule (glutaraldehyde). A molecular layer with amine terminations ( $-\text{NH}_2$ ) is formed on the sensor surface by a process referred to as silanisation and it is carried out using APTES. The linker molecule (glutaraldehyde), in principle, can covalently bond with the amine terminations forming imine ( $\text{C}=\text{N}$ ) linkages. Enzymes are immobilised first by silanising the sensor surface followed by treating the sensor surface with activated glutaraldehyde and lipase.<sup>22</sup> The process is initiated by activating the nitride surface with a  $\text{N}_2\text{O}$  plasma<sup>23</sup> in a PECVD system. This results in the formation of  $-\text{OH}$  bonds on the surface of the nitride. The  $\text{N}_2\text{O}$  plasma treatment helps to promote uniform covalent adhesion of APTES and other subsequent functional layers to the nitride surface of the sensor.<sup>24</sup> The sensors are

treated in  $\text{N}_2\text{O}$  plasma for 5 minutes in the PECVD system at 250  $^\circ\text{C}$ . Plasma enhanced sensors are immediately transferred to 1% APTES in anhydrous toluene (v/v) and allowed to react at 70  $^\circ\text{C}$  for 1 hour. The wafers after the APTES treatment are rinsed gently thrice in toluene, ethanol and DI water respectively to remove any adsorbed molecules on the surface. Subsequently, the samples after curing at 120  $^\circ\text{C}$  for 10 minutes are treated with 0.5% glutaraldehyde in DI water (v/v) for 2 hours at room temperature and again cured at 120  $^\circ\text{C}$  for 10 minutes. Batch processing is carried out until this step to get maximum process matching among the sensors. After this step, individual sensors are diced out using an Ultra slice dicing machine (Ultra Tech Manufacturing, USA) to singulate the sensors. The active device area (microreactors) of the sensor is protected using parafilm® wax and clean room tape while dicing the wafer. The sensor surface is treated with the enzyme (lipase) after integrating the counter electrode with the sensor.

The procedure of counter electrode integration with the sensor has been reported in our previous work.<sup>20,21</sup> Briefly, through holes of 3 mm diameter are etched in the boro-float glass wafers with 49% electronic grade HF acid. Thick photoresists and Cr-Au act as masking layers. After removing any residue, the glass wafers are diced out before depositing on the counter electrode. A thin film Ag-AgCl electrode is formed on the through hole etched glass wafer by depositing Ag with Cr-Au as pre-layers in a vacuum e-beam metallisation (HindHivac, India) system. AgCl is electrochemically deposited on the Ag layer. The singulated glass and the silicon wafers are bonded together using a photoresist as an adhesive material. After bonding the glass and silicon wafers, the device active area (microreactors) is activated in 3  $\mu\text{l}$  of lipase (1 mg  $\text{ml}^{-1}$ ) in Tris-HCl buffer (200 mM, pH 7.2) for 24 hours. The samples are finally washed thoroughly with DI water to remove any adsorbed enzyme. Fig. 1(a) shows with dimensions the structure of the large area EISCAP used in our previous work<sup>18</sup> where the electrolyte (blood serum sample and free enzyme) was held in a Teflon® cell and a platinum (Pt) wire dipped in the electrolyte was used as a counter electrode. The schematic of the miniaturised EISCAP TG biosensor with dimensions marked is shown in Fig. 1(b). The stages of immobilising the enzyme (lipase) to the nitride surface are shown in Fig. 1(c). Fig. 2(a) shows the photograph of the singulated sensor covered with parafilm wax® and clean room tape. Fig. 2(b) shows the photograph of the final sensor with dimensions marked.

### 2.3 Biochemical characterisation and calibration

The activity of the enzyme *P. cepacia* lipase after purification is determined by *p*NPB assay as reported.<sup>25,26</sup> The Michaelis constants  $K_m$  (shown in Fig. 3) for free and immobilised enzyme kinetics measured at half of the maximum enzyme velocity at the maximum substrate concentration ( $V_{\text{max}}/2$ ) are found to be 27.97  $\mu\text{M}$  and 36.48  $\mu\text{M}$ . The specific activities of the free and immobilised enzyme kinetics are found to be 37.8 U  $\text{mg}^{-1}$  and 28.95 U  $\text{mg}^{-1}$  (one enzyme unit 'U' is defined as the amount of enzyme that converts 1  $\mu\text{M}$  of *p*NPB into product per minute). The immobilised enzyme retained 76.58% of its native activity. Fig. 3

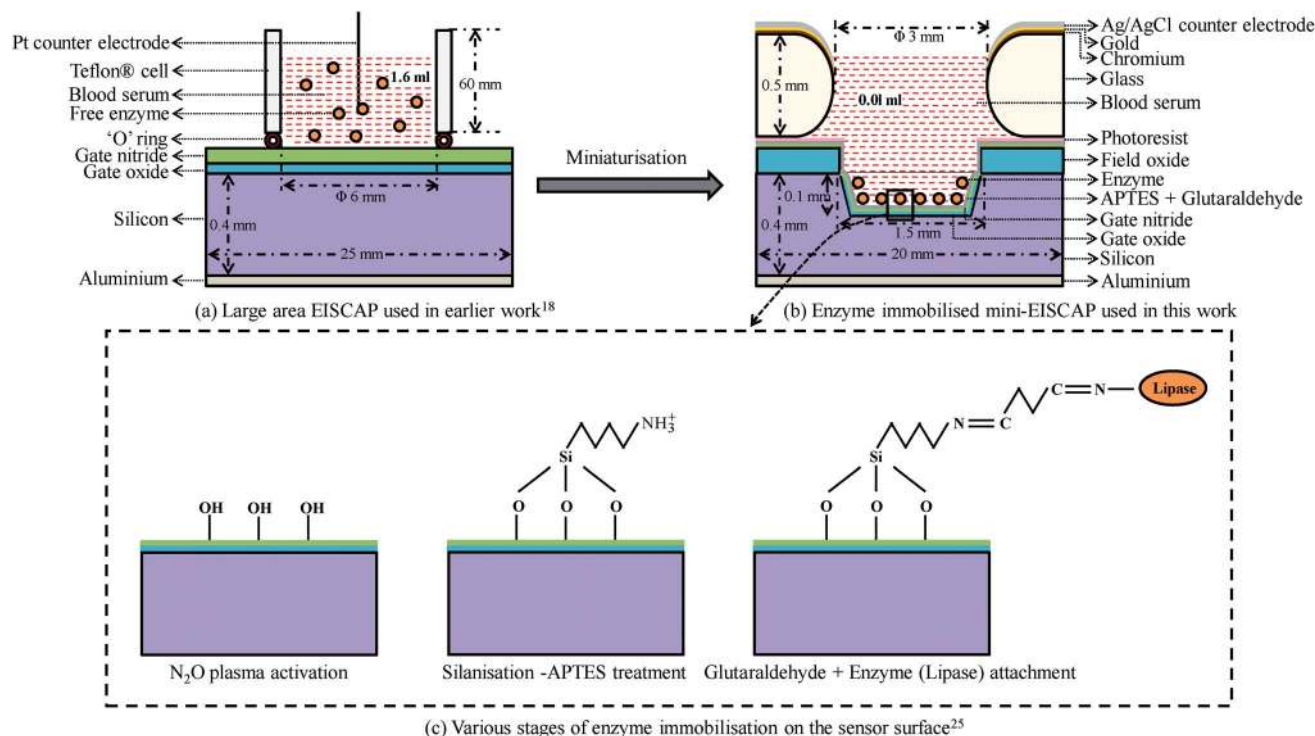


Fig. 1 Schematic of a miniaturised EISCAP TG biosensor (not drawn to scale).

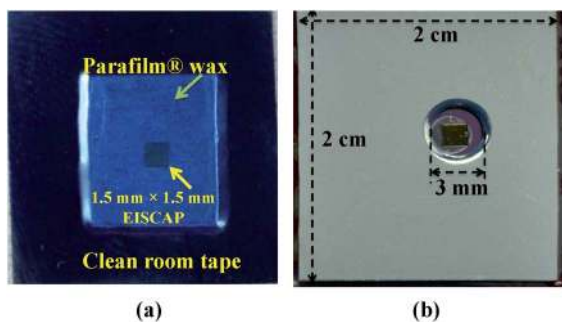


Fig. 2 Photographs of (a) the diced sensor covered with parafilm® and clean room adhesive tape and (b) singulated bonded and enzyme immobilised EISCAPs.

shows the rate of the enzymatic reactions of free and immobilised enzyme. The percentage of specific activity of immobilized enzyme relative to that of free enzyme varies from 70% to 80% between different chips that are batch processed. The Fourier transform infrared (FTIR) spectra measured as reported previously<sup>25</sup> confirm the formation of hydroxyl, amine and imine bonds after each of the immobilisation process steps. The details of the enzyme assay and FTIR are mentioned in the ESI.†

The TG concentration in blood serum is measured based on the information on the rate of TG hydrolysis (calibration point). Tributyrin, a standard TG is used in this experiment. Tributyrin concentrations varying from 0.5 mM to 1.5 mM in steps of 0.25 mM are prepared using Tris-HCl buffer (pH 7.2) and acetonitrile as a co-solvent. The co-solvent plays a major role in mixing the tributyrin homogeneously in the buffer. A buffer is necessary to

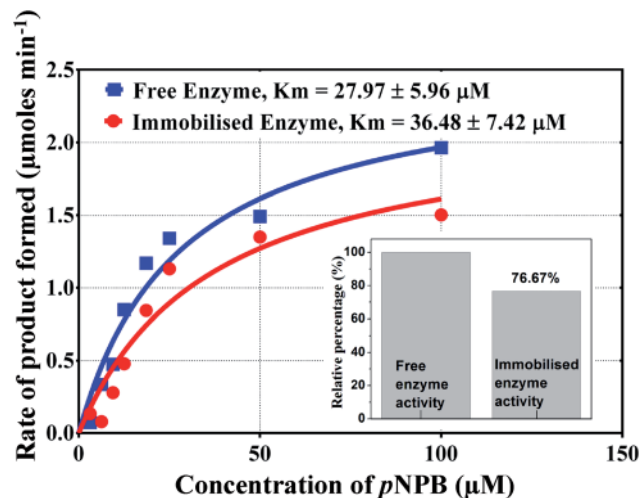


Fig. 3 Free and immobilised enzyme activity plots. The inset shows the percentage of specific activity of the immobilised enzyme relative to that of the free enzyme.

provide a suitable environment for optimal enzyme activity. In our previous work,<sup>18</sup> we have optimised the buffer concentration of phosphate buffer to be 0.25 mM at pH 6. However, with this buffer, it was not possible to determine the final pH at a lower substrate concentration such as 1 mM tributyrin that is critical in clinical applications. Hence, in the improved version, we adopted the Tris-HCl buffer system. The rate of tributyrin hydrolysis is measured using a pH meter. The inset in Fig. 4 shows the measured pH change with time for different

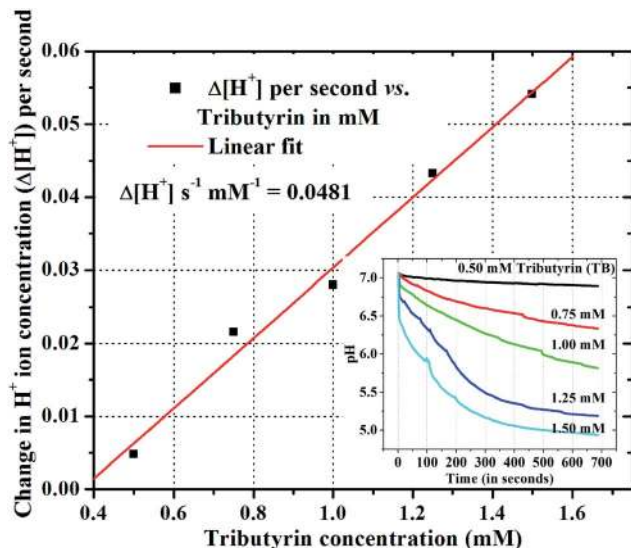


Fig. 4 Tributyrin standard plot—average rate of hydrolysis measured at different time instances between 1 and 2 minutes of the enzymatic reaction<sup>21</sup> is found to be  $0.0481 [\text{H}^+] \text{ s}^{-1} \text{ mM}^{-1}$ . The inset shows the pH change with time due to hydrolysis of tributyrin of different concentrations with lipase.

tributyrin concentrations. A standard plot (Fig. 4) of the average rate of tributyrin concentration vs.  $[\text{H}^+]$  ion concentration measured between 1 and 2 minutes of hydrolysis is obtained from the pH vs. time graph measured using a pH meter. The interval of 1 to 2 minutes is chosen to confine the measurement to the linear region of the enzyme kinetics. The biochemical sensitivity ( $S_{\text{std}}$ ) from the standard plot of the tributyrin is measured to be  $0.0481 [\text{H}^+] \text{ s}^{-1} \text{ mM}^{-1}$  or  $0.00481 \text{ pH s}^{-1} \text{ mM}^{-1}$ .

#### 2.4 TG measurement protocols

The principle of readout of TG in blood serum is fundamentally similar to the pH readout system reported previously.<sup>20</sup> In our previous work, we used pH 4 and pH 8 as reference electrolytes to calibrate the sensor against process variations. In this work, the TG measurement is performed on an enzyme immobilised sensor and hence, the standard pH reference solution of pH 4 cannot be used as the enzyme activity could be deteriorated at this pH. Hence, the reference pH solutions for the TG readout system are chosen to be pH 6 and pH 8.5 and they are used in calibrating the sensor against process variations using (1). The readout circuit and the protocol for the measurement of TG in blood serum are implemented using a mixed signal embedded chip from Cypress semiconductors (PSoC3®, CY8C3866AXI-040)<sup>27</sup> with minimal external components on a compact custom made printed circuit board of size 11 cm x 6 cm. The readout circuit principle and the details of the calibration and measurement protocols are discussed in the ESI.† The calibration and measurement modes are shown in Fig. 5 using the EISCAP  $C-V$  characteristics.

$$\Delta V_{\text{ref}} = 59.2\alpha(\text{pH } 8.5 - \text{pH } 6) \quad (1)$$

The TG under test is measured as follows.

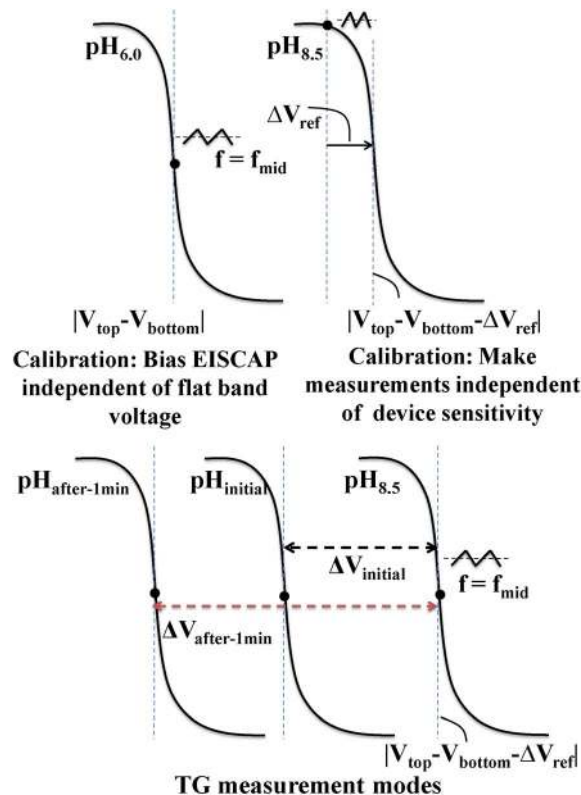


Fig. 5 Calibration and measurement modes using  $C-V$  curves.

- The sensor is calibrated by biasing it in the middle of the  $C-V$  curve (where EISCAP produces  $f = f_{\text{mid}}$  clock frequency) and by measuring the pH sensitivity ( $\Delta V_{\text{ref}}/2.5$ ) using pH 6 and pH 8.5 electrolytes to account for the variations in the flat band voltage and the device sensitivity. The voltage shift (in mV) corresponding to a change in the pH from 6 to 8.5 at 25 °C (in mV) is given as (rewriting (1)):

$$\Delta V_{\text{ref}} = 59.2\alpha(\text{pH } 8.5 - \text{pH } 6) \quad (2)$$

- The biochemical sensitivity from the standard plot discussed in sub-section 2.3 ( $S_{\text{std}}$  after 1 minute duration) is given as

$$S_{\text{std}_1\text{min}} = 0.28 \text{ pH/mM} \quad (3)$$

- pH sensitivity ( $S$ , in mV/ $\Delta\text{pH}$ ) of the device is calculated from (2):

$$S = \Delta V_{\text{ref}}/2.5 \quad (4)$$

- The blood serum sample, whose TG is to be determined, is placed in the sensor. The initial voltage and the voltage after 1 minute to bring back the frequency of oscillation to  $f_{\text{mid}}$  are measured. The voltage shift ( $\Delta V_{\text{test\_TG}} = \Delta V_{\text{after\_1min}} - \Delta V_{\text{initial}}$ ) corresponds to the rate of hydrolysis depending on the concentration of the TG present in the blood serum in a one minute interval.

$$\Delta V_{\text{test\_TG}} = 59.2\alpha(\text{pH}_{\text{initial}} - \text{pH}_{\text{after\_1min}}) \quad (5)$$

• From (3)–(5),  $S_{\text{std}_1\text{min}}$ ,  $S$ , and  $\Delta V_{\text{test-TG}}$ , the unknown concentration of TG in the blood serum is estimated to be:

$$\text{TG (in mM)} = \Delta V_{\text{test-TG}} / (S \times S_{\text{std}_1\text{min}}) \quad (6)$$

• The unknown TG in blood serum is now determined using (6). The result of the test TG is displayed on the LCD screen.

## 3 Results and discussion

### 3.1 Blood serum TG measurements

The miniaturised EISCAP TG sensors are tested using blood serum samples to estimate the TG content. Blood samples were taken from volunteers of both sexes in the age group from 20 to 35 years. The samples were collected at the IIT Madras institute

hospital after obtaining ethical clearance. One part of the collected sample was tested for TG in the clinical laboratory and the other part was used in this study to validate the miniaturised EISCAP sensors. The serum samples of 10  $\mu\text{l}$  are delivered to the device using a micropipette.

Fig. 6–9 show typical  $C$ – $V$  plots measured on miniaturised EISCAP sensors using an Agilent E4980A LCR meter. The TG measurement protocol discussed in sub-section 2.4 is used to estimate the blood serum TG concentration. The measurement procedure is discussed taking examples of sensor D1 with blood serum sample A and sensor D2 with blood serum sample B. The pH sensitivity of sensor D1 is measured by calibrating it using two reference pH solutions (pH 6 and pH 8.5) and it is found to be 35.35 mV per pH unit. After placing blood serum sample A in D1, the shift  $\Delta V_{\text{test-TG}}$  ( $= \Delta V_{\text{after 1 min}} - \Delta V_{\text{initial}}$ , indicated in Fig. 5) in the  $C$ – $V$  curve from the moment the sample is placed to the end of the 1 minute interval is measured to be 19.1 mV.

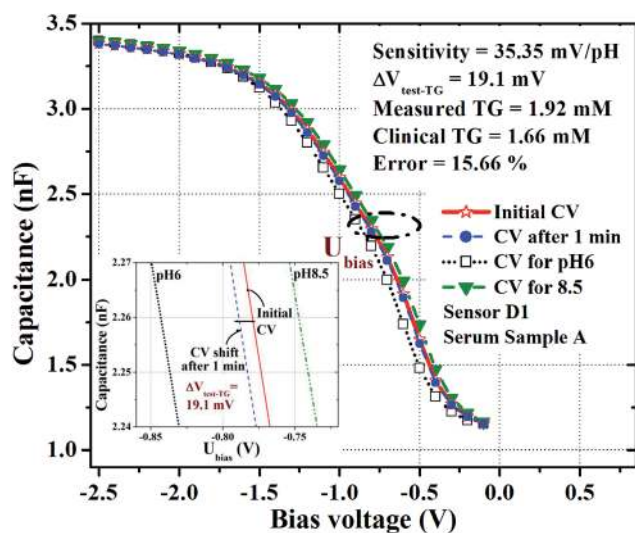


Fig. 6  $C$ – $V$  plots showing the device sensitivity and the TG hydrolysis in sensor D1 with blood serum A.

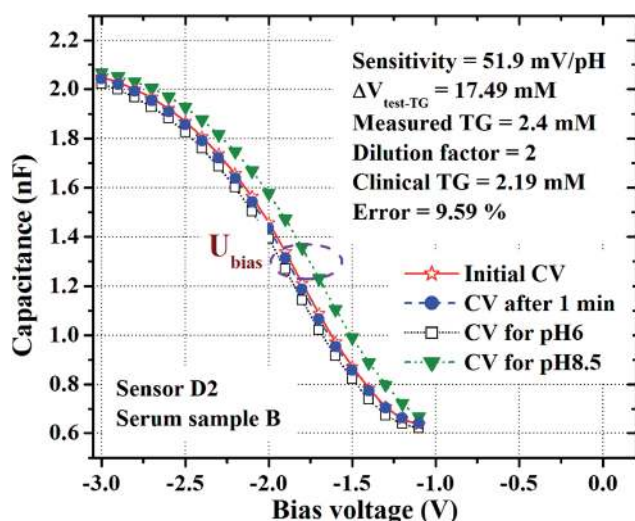


Fig. 7  $C$ – $V$  plots showing the device sensitivity and the TG hydrolysis in sensor D2 with blood serum B after diluting with Tris–HCl buffer.

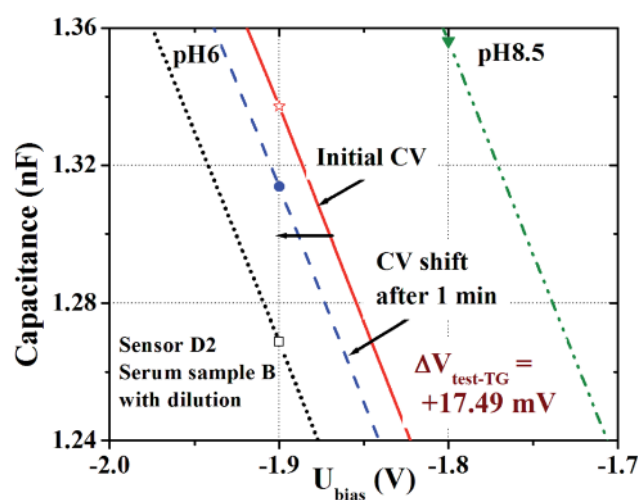


Fig. 8 Enlarged plots of  $C$ – $V$  measurements (at the mid-point of the  $C$ – $V$ ) on sensor D2 with no dilution of buffer with blood serum B.

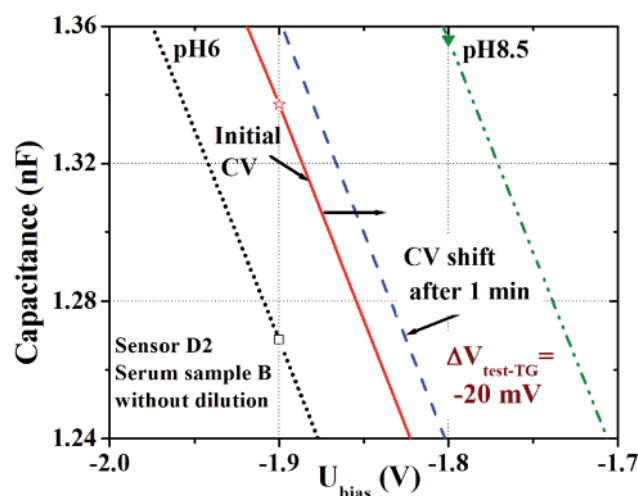


Fig. 9 Enlarged plots of  $C$ – $V$  measurements (at the mid-point of the  $C$ – $V$ ) on sensor D2 with dilution of buffer with blood serum B.

Table 1 Comparison of triglyceride concentrations in blood samples measured using EISCAP and a CV meter with clinical data

Sensor	Serum sample	Blood serum dilution with Tris-HCl buffer pH 7.4	Device sensitivity ( $S = \Delta V/\text{pH}$ )	$\Delta V_{\text{test\_TG}}$ (mV)	Measured TG (mM)	Clinical TG (mM)	% Error
D1	A	No dilution	35.35	+19.10	1.92	1.66	15.66
D2	B	No dilution	51.90	-20.00	—	2.19	—
D2	B	1 : 1	51.90	+17.49	2.40	2.19	09.59

The inset in Fig. 6 clearly shows a shift in the  $C-V$  curve after 1 minute to the left of the initial  $C-V$  curve confirming the hydrolysis of the TG in blood serum. From  $S_{\text{std\_1min}}$ ,  $S$ , and the shift  $\Delta V_{\text{test\_TG}}$  (+19.1 mV), the concentration of TG in serum sample A is estimated to be 1.92 mM. The clinical lab measurement was 1.66 mM for the same serum sample A.

Some blood serum samples exhibit negative  $\Delta V_{\text{test\_TG}}$  values and have to be diluted with Tris-HCl buffer (pH 7.4) to bring them within the clinical range 0.56–1.68 mM (50–150 mg dL<sup>-1</sup>, unit conversion: 1 mM ~ 89 mg dL<sup>-1</sup>). The dilution is necessary to reduce the effect of the buffering action of blood<sup>28</sup> which is more rapid when the amount of TG in blood is higher than the normal clinical range. A negative value of  $\Delta V_{\text{test\_TG}}$  indicates that the  $C-V$  curve after 1 minute of TG hydrolysis shifts to the right of the initial  $C-V$  curve, due to the rapid buffering action of blood buffer within a minute time interval. An example of

higher TG measurement (device D2, serum sample B, Fig. 7) details is discussed as follows. The pH sensitivity of sensor D2 is measured by calibrating it using two reference pH solutions (pH 6 and pH 8.5) and it is found to be 51.9 mV per pH unit. After placing blood serum sample B in D2, the shift ( $\Delta V_{\text{test\_TG}}$ ) in the  $C-V$  curve (Fig. 8) from the moment the sample is placed to the end of the 1 minute interval results in a negative  $\Delta V_{\text{test\_TG}}$  value (-20 mV) confirming the rapid blood buffering action. Fig. 9 shows the hydrolysis of the same sample after diluting it with Tris-HCl buffer (pH 7.4) solution. The shift in the  $C-V$  curve after 1 minute of TG hydrolysis is positive  $\Delta V_{\text{test\_TG}}$  (+17.49 mV), confirming that the rapid buffering action of the blood initiated by the high TG concentration has been mitigated. Table 1 shows the comparison of TG concentrations in blood serum (A and B) measured using our sensors (D1 and D2) with the pathology laboratory data.

Fig. 10 shows the photograph of the TG readout system connected with the mini-EISCAP. The nominal frequency of the EISCAP relaxation oscillator is set to be 4 kHz and the PSoC® system clock frequency is set to be 10 MHz. The mini-EISCAP is kept in a black box that prevents light from interfering with sensor measurements and has a provision to connect the top and bottom contacts of the sensor to the readout system as shown in Fig. 10. Table 2 compares the readout measured TG against the clinically measured TG and it gives data on the device sensitivity and  $C-V$  shift ( $\Delta V_{\text{test\_TG}}$ ) after 1 minute of hydrolysis. If the measured  $\Delta V_{\text{test\_TG}}$  is negative then the readout system indicates the need for dilution of the blood serum with Tris-HCl buffer (pH 7.4) in a 1 : 1 ratio. A multiplication factor of 2 is automatically used to calculate the TG value when the diluted sample is used for testing. The error obtained from the TG readout measurements (Table 2) varies from 7.79 to 16.66%. The EISCAP device sensitivity and the

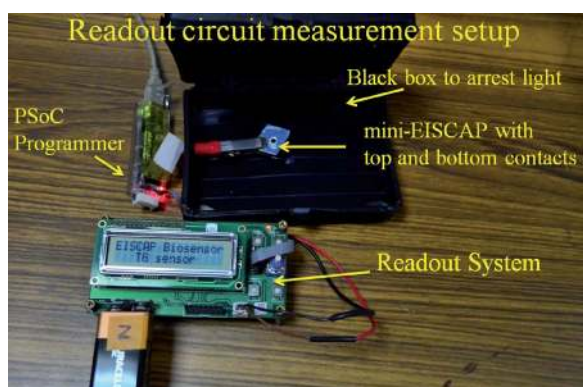


Fig. 10 Photograph of the readout measurement setup with a packaged miniaturised EISCAP sensor.

Table 2 Comparison of TG concentrations in blood serum samples measured using the readout system with clinical data

Sample/sensor no.	Age group	Blood serum dilution with Tris-HCl buffer pH 7.4	Device sensitivity ( $S = \Delta V/\text{pH}$ )	$\Delta V_{\text{test\_TG}}$ (mV)	Measured TG (mM)	Clinical TG (mM)	% Error
1	20–25	No dilution	57.0	34.6	2.17	1.86	16.66
2	20–25	No dilution	45.3	10.5	0.83	0.77	07.79
3	20–25	No dilution	53.3	11.5	0.77	0.71	08.45
4	20–25	1 : 1	49.4	18.7	2.70	2.42	11.57
5	26–30	No dilution	48.2	20.9	1.55	1.43	08.39
6	26–30	No dilution	47.0	25.3	1.92	1.66	15.66
7	26–30	1 : 1	48.9	16.6	2.42	2.24	08.03
8	31–35	No dilution	39.6	19.2	1.73	1.50	15.33
9	31–35	No dilution	40.2	17.5	1.55	1.39	11.51
10	31–35	1 : 1	50.1	21.9	3.12	2.86	09.09

Table 3 Comparison of analytical parameters of the large EISCAP (previous work)<sup>18</sup> and the miniaturised EISCAP (present work)

Parameters	Large EISCAP – previous work <sup>18</sup>	Miniaturised EISCAP – present work
Blood serum sample volume	80 $\mu\text{l}$	5 to 10 $\mu\text{l}$
Buffer and enzyme	Phosphate buffer (pH 6), 0.25 mM; <i>P. cepacia</i> lipase – free enzyme	Tris-HCl buffer (pH 7.4), 200 mM; <i>P. cepacia</i> lipase – immobilized enzyme
Total solution volume	1.6 ml	10 $\mu\text{l}$
Device sensitivity (minimum–maximum)	30–55 mV per pH unit	35.35–57 mV per pH unit
Clinical TG reported	1.9 to 2.9 mM	0.7 to 2.86 mM
Surface area to volume ratio ( $\text{mm}^2 \mu\text{l}^{-1}$ )	0.0177	0.285
Measurement time	30 minutes + post processing time	Total readout time is within 5 minutes
Handling	Complex since the enzyme and counter electrode are not integrated with the sensor. Post-processing is required to determine the unknown TG	Simple since the enzyme and counter electrode are integrated with the sensor. The readout system determines and displays the unknown TG

Table 4 Comparison of analytical parameters between some of the reported TG biosensors

Type	Immobilisation mechanism	Type of electrode	Detection limit	Linear range	Response time	Shelf life	Ref.
Amperometric	Polyvinyl alcohol–glutaraldehyde cross-linkage	Pt	0.21 mM	0.56 to 2.25 mM	2 s	50% loss in 70 days	29
Electrochemical	ZnO nanoparticles – covalent cross-linkage	Pt	20 mg $\text{dL}^{-1}$	50 to 650 mg $\text{dL}^{-1}$	6 s	50% loss in 70 days	30
Electrochemical	Conducting polymer (gold polypyrrole) – covalent linkage	Au	20 mg $\text{dL}^{-1}$	50 to 700 mg $\text{dL}^{-1}$	4 s	50% loss in 70 days	31
Potentiometric	External immobilisation – enzyme attached to a separate reactor	Ion sensitive FET	Not reported	5 to 30 mM	<5 min	45% loss in 2 weeks	10
Potentiometric	Glutaraldehyde cross-linkage – immobilisation on the sensor surface	EISCAP	0.5 mM	0.7 to 2.86 mM	<5 min	30% loss in 2 weeks	Present work

enzyme activity play a major role in appropriate measurement of the TG concentration. The reduction in either of the sensitivities could be the reason for the measured error. The device sensitivity depends on the  $-\text{NH}_2$  bonds on the surface of the nitride layer, but they get replaced by  $-\text{OH}$  bonds due to the surface hydration by the electrolyte. The enzyme activity could be affected by non-uniform surface functionalisation. The enzyme activity depends on the active site orientation on the functionalised surface and this could vary from device to device.

### 3.2 Comparison of the present work with previous studies

Miniaturisation of EISCAPs has led to one order of magnitude improvement in the surface area to volume ratio compared to the large EISCAP, thereby increasing the device sensitivity. The device dimensions of the large area EISCAP<sup>18</sup> and the miniaturised EISCAP are shown in Fig. 1. The volume of the electrolyte that can be held by the miniaturised EISCAP before packaging is 0.2  $\mu\text{l}$  and after packaging is 10  $\mu\text{l}$ , while that of the Teflon® cell held large EISCAP<sup>18</sup> was 1.6 ml and hence there is 160 times reduction in the total volume of the electrolyte. The through hole in the glass wafer not only helps in containing the electrolyte, but also ensures the contact of electrolyte with the thin film electrode in the side walls. Miniaturisation can help in improving the uniformity in enzyme immobilisation among batch processed EISCAP devices. But the immobilised enzyme activity depends on the availability of the enzyme active sites for

the hydrolysis of TG. A comparative study of our present and previous work is given in Table 3. Comparisons between some of the reported strategies<sup>29–32</sup> and the present work are given in Table 4. Compared to other strategies this work presents the design of a TG biochip with an integrated enzyme and counter electrode along with a compact readout system to measure and display the unknown TG concentration in blood serum within a reasonable time duration of 5 minutes. In this strategy, it is possible to make an array of miniaturised EISCAP biosensors on silicon to monitor various blood compositions on a single chip.

## 4 Conclusions

Miniaturised EISCAP biosensors that use enzymatic hydrolysis to detect triglyceride in blood serum are batch processed with optimised process steps to improve the device and the biochemical sensitivity. The miniaturised sensors are fabricated on silicon wafers and are bonded to the through hole etched glass wafers using a photoresist as an adhesive at room temperature. Enzyme *P. cepacia* lipase is immobilised on the surface of the sensor and the activity of the enzyme is quantified using biochemical assay. A compact electronic readout system is designed using a custom made printed circuit board and PSOC® chip from Cypress semiconductors. The enzyme immobilised miniaturised sensor is embedded in a successive approximation analog to digital conversion algorithm to calibrate the sensor

and to measure the triglyceride concentration in blood serum and display the same within 5 minutes. The integrated sensor along with an electronic readout system is used for sensing and estimating the triglyceride concentration in blood serum samples and the results are compared with the clinical lab data. The device sensitivity of the miniaturised devices that we measured varies between 35.35 and 57.00 mV per pH unit. The error obtained from the TG readout measurements varies between 7.79 and 16.66% and this could be because of the reduction in the device sensitivity or enzyme activity in the final sensor. The miniaturised EISCAP sensors are designed to detect and estimate the amount of TG present in blood serum within the clinical range of 50 to 150 mg dL<sup>-1</sup>. This type of biosensor is of relevance to the biomedical and food industries. The sensor can also work for other bio-analytes like urea and glucose with appropriate enzymes and change in the calibration and measurement algorithm to suit specific applications.

## Acknowledgements

We acknowledge the National Programme on MEMS And Smart Structures (NPMASS), India for the financial support. Experimental work was carried out at the Centre for NEMS and Nanophotonics, IIT Madras sponsored by the Department of Electronics and Information Technology, India. We also thank Prof. Shanthi Pavan, Department of Electrical Engineering, IIT Madras for valuable suggestions.

## References

- 1 A. Hierlemann, D. Lange, C. Hagleitner, N. Kerness, A. Koll, O. Brand and H. Baltes, *Sens. Actuators, B*, 2000, **70**(13), 2–11.
- 2 C. S. Pundir and J. Narang, *Int. J. Biol. Macromol.*, 2013, **61**, 379–389.
- 3 A. Phongphut, C. Sriprachubwong, A. Wisitsoraat, A. Tuantranont, S. Prichanont and P. Sritongkham, *Sens. Actuators, B*, 2013, **178**, 501–507.
- 4 J. Narang, N. Chauhan and C. S. Pundir, *Int. J. Biol. Macromol.*, 2013, **60**, 45–51.
- 5 J. Narang and C. S. Pundir, *Int. J. Biol. Macromol.*, 2011, **49**(4), 707–715.
- 6 S. Setzu, S. Salis, V. Demontis, A. Salis, M. Monduzzi and G. Mula, *Phys. Status Solidi A*, 2007, **204**(5), 1434–1438.
- 7 A. Vijayalakshmi, Y. Tarunashree, B. Baruwati, S. V. Manorama, B. L. Narayana, R. E. C. Johnson and N. M. Rao, *Biosens. Bioelectron.*, 2008, **23**(11), 1708–1714.
- 8 M. Nakako, Y. Hanazato, M. Maeda and S. Shiono, *Anal. Chim. Acta*, 1986, **185**, 179–185.
- 9 M. J. Schoning, A. Kurowski, M. Thust, P. Kordos, J. W. Schultze and H. Luth, *Sens. Actuators, B*, 2000, **64**, 59–64.
- 10 D. G. Pijanowska, R. Wiater, G. Ginalska, J. Lobarzewski and W. Torbicz, *Sens. Actuators, B*, 2001, **78**, 263–266.
- 11 P. Bergveld, *IEEE Trans. Biomed. Eng.*, 1970, **17**, 70–71.
- 12 P. Bergveld, *IEEE Trans. Biomed. Eng.*, 1972, **19**, 342–351.
- 13 I. Basu, R. V. Subramanian, A. Mathew, A. M. Kayastha, A. Chadha and E. Bhattacharya, *Sens. Actuators, B*, 2005, **107**, 418–423.
- 14 W. M. Siu and R. S. C. Cobbold, *IEEE Trans. Electron Devices*, 1979, **26**, 1805–1815.
- 15 R. Ravi Kumar Reddy, I. Basu, E. Bhattacharya and A. Chadha, *Curr. Appl. Phys.*, 2003, **3**, 155–161.
- 16 R. Ravi Kumar Reddy, A. Chadha and E. Bhattacharya, *Biosens. Bioelectron.*, 2001, **16**, 313–317.
- 17 V. Hareesh, R. E. Fernandez, E. Bhattacharya and A. Chadha, *J. Mater. Sci.: Mater. Med.*, 2009, **20**(suppl. 1), 229–234.
- 18 R. Preetha, K. Rani, M. S. S. Veeramani, R. E. Fernandez, H. Vemulachedu, M. Sugan, E. Bhattacharya and A. Chadha, *Sens. Actuators, B*, 2011, **160**(1), 1439–1443.
- 19 V. Hareesh, S. Pavan and E. Bhattacharya, *IEEE BioCAS*, 2008, 73–76.
- 20 M. S. Veeramani, P. Shyam, N. P. Ratchagar, A. Chadha, E. Bhattacharya and S. Pavan, *IEEE Sens. J.*, 2013, **13**(5), 1941–1948.
- 21 M. S. Veeramani, P. Shyam, N. P. Ratchagar, A. Chadha, E. Bhattacharya and S. Pavan, *IEEE Sensors Conference*, 2013, 3–6.
- 22 J. A. Howarter and J. P. Youngblood, *Langmuir*, 2006, **22**(26), 11142–11147.
- 23 M. Bose, D. K. Basa and D. N. Bose, *Appl. Surf. Sci.*, 2000, **158**(3–4), 275–280.
- 24 L.-T. Yin, J.-C. Chou, W.-Y. Chung, T.-P. Sun, S.-K. Hsiung, L.-T. Yin and J.-C. Cha, *IEEE Trans. Biomed. Eng.*, 2001, **48**(3), 340–344.
- 25 R. E. Fernandez, E. Bhattacharya and A. Chadha, *Appl. Surf. Sci.*, 2008, **254**(15), 4512–4519.
- 26 K. Shirai and R. L. Jackson, *J. Biol. Chem.*, 1982, **257**(3), 1253–1258.
- 27 *Cypress Semiconductors PSOC3 datasheet*, Cypress Semiconductors Pvt. Ltd., San Jose, CA, 1982, <http://www.cypress.com/go/psoc3>.
- 28 D. L. Nelson, M. M. Cox, *Lehninger principles of biochemistry*, WH Freeman, 2010.
- 29 C. S. Pundir, S. S. Bharvi and J. Narang, *Clin. Biochem.*, 2010, **43**, 467–472.
- 30 J. Narang and C. S. Pundir, *Int. J. Biol. Macromol.*, 2011, **49**, 707–715.
- 31 J. Narang, N. Chauhan, P. Rani and C. S. Pundir, *Bioprocess Biosyst. Eng.*, 2013, **36**, 425–432.
- 32 C. S. Pundir and J. Narang, *Int. J. Biol. Macromol.*, 2013, **61**, 379–389.